Geometry from local flatness in Lorentzian spin foam theories

Pietro Donà[*]

Center for Space, Time and the Quantum, 13288 Marseille, France Department of Physics and Astronomy, University of Western Ontario, London, Ontario N6A 5B7, Canada

Local flatness is a property shared by all the spin foam models. It ensures that the theory's fundamental building blocks are flat by requiring locally-trivial parallel transport. In the context of simplicial Lorentzian spin foam theory, we show that local flatness is the main responsible for the emergence of geometry independently of the details of the spin foam model. We discuss the asymptotic analysis of the Engle-Pereira-Rovelli-Livine spin foam amplitudes in the large quantum number regime, highlighting the interplay with local flatness.

I. INTRODUCTION AND MOTIVATIONS

Spin foam theory is a promising candidate for quantization of gravity and is often referred to as the covariant formulation of loop quantum gravity. It attempts to define a Lorentzian background-independent path integral for general relativity regularized on a fixed triangulation of a spacetime manifold. The theory assigns quantum numbers representing geometric quantities to the 2-complex dual to the triangulation. The path integral sums over all the possible quantum numbers describe a sum over quantum geometries. Moreover, spin foam theory assigns transition amplitudes to states in the kinematical Hilbert space of loop quantum gravity associated with the triangulation boundary.

The Engle-Pereira-Rovelli-Livine/Freidel-Krasnov (EPRL/FK) model [1,2] is the most promising spin foam theory available that is currently being developed (see [3,4] for a pedagogical introduction). Its most celebrated and successful result is the emergence of Regge geometries and the Regge action in the large quantum numbers regime of the spin foam amplitudes [5]. There are many extensions and applications including but not limited to the Euclidean EPRL model [6], the topological $SU(2)$ BF theory [7,8], to general cellular decomposition known as the KKL model [9,10], to generic $SL(2, \mathbb{C})$ tensors [11], and have a numerical confirmation [12,13]. The original and the majority of the related works are based on the bivector reconstruction theorem [14] a map from Euclidean or Lorentzian 4-simplices to a collection of bivectors satisfying (linear simplicity) constraints. This elegant theorem was instrumental in driving the geometrical intuition of spin foam models, and Regge calculus is the best tool to study the semiclassical limit [15,16].

The EPRL spin foam model, and all of its extensions, have very complicated recipes with many components mixed. The traditional semiclassical analysis of the EPRL spin foam model does not disentangle the role played by each ingredient and blends all of them. A clear picture of each contribution is fundamental to proposing improvements, extensions, and generalizations of the model and increasing our understanding of the theory. We separate the analysis into two main components; the *local flatness* of the spin foam vertices and the role of *saddle-point* equations.

We abandon the bivector reconstruction theorem favoring gauge covariant geometrical objects like framed polyhedra, dihedral angles, and twist angles. This description follows, and is inspired by, previous work on discrete holonomy-flux geometries [17] and on twisted geometries [18–21]. We parametrize the wedge holonomies using a set of four framed planes for each edge and a complex angle to each wedge.

Spin foam models are built with *locally flat* triangulations. Any parallel transport in a 4-simplex is trivial. This property is very general, and all the spin foam models in the literature share it. When we impose *local flatness* to a set of general holonomies, we find that geometry naturally emerges. The holonomies are Regge-like. Since local flatness does not involve areas, we cannot expect to reconstruct a full Regge geometry. The holonomies contain information on just the angles of the emerging geometry. Suppose we also provide a closure condition for each edge. In that case, we can identify framed tetrahedra and a unique Regge geometry emerge up to a scale factor (if we ignore the topological sector and discrete symmetries). This result is entirely independent of the details of the model itself. Therefore, we expect the emergence of geometry to be a typical result of all locally-flat spin foam models.

We study the large quantum number regime of the EPRL spin foam amplitude with *saddle-point* techniques. The resulting equations provide a closure equation to each edge and align the boundary framed planes with the ones parametrizing the wedge holonomies. As a result, at the saddle

[*]dona.pietro@gmail.com

066011-1

point, the amplitude assumes a simple form in terms of the complex angles of the wedge holonomies mixing boost and rotation angles with the Immirzi parameter. Only if local flatness is considered the saddle point action assumes the form of the Regge action completing the connection with discrete general relativity.

As a coproduct of our study, we provide an explicit form of the action at the saddle point in terms of gauge invariant quantities. In particular, its imaginary part was not studied enough in the literature (because it is usually deemed as irrelevant [5] or gauge fixed [12]). However, having complete control of all the phases is necessary for the numerical evaluation of the amplitude [12,22].

We complete our analysis by also studying the case of extended triangulations with many vertices. First, we consider them fixed and large instead of summing over the bulk quantum numbers. The saddle-point equations reduce to a closure condition at every edge and gluing equations that tell us how to glue the geometry of the various vertices together. We complement the analysis by looking at the role of the sum over bulk degrees of freedom. We follow the seminal work of [23] and find that the face holonomy is constrained to be a 4-screw with proportional boost and rotation angles. The naive flatness problem arises immediately if this condition is supplemented by local flatness and gluing conditions.

II. SPINORS, FRAMED PLANES AND MAPS BETWEEN THEM

Spinors are elements of the vector space $\mathbb{C}^2$. We indicate a spinor and its conjugate transpose with $|z\rangle$ and $\langle z|$.

$$|z\rangle := \begin{pmatrix} z_0 \\ z_1 \end{pmatrix}, \qquad \langle z| := (\bar{z}_0, \bar{z}_1). \qquad (1)$$

We use the Dirac notation to simplify the bookkeeping of spinorial indices. The spinorial space comes with a natural inner product given by $\langle w|z\rangle := \bar{w}_0 z_0 + \bar{w}_1 z_1$ and a duality map $\mathcal{J}: \mathbb{C}^2 \to \mathbb{C}^2$

$$\mathcal{J}|z\rangle = |z] := \begin{pmatrix} -\bar{z}_1 \\ \bar{z}_0 \end{pmatrix}. \qquad (2)$$

Moreover, a spinor and its dual form an orthogonal basis of $\mathbb{C}^2$. Spinors also have many interesting properties useful for performing calculations. We report some of them in Appendix A.

A spinor naturally defines also a basis of $\mathbb{R}^3$ given by $(\vec{n}, \vec{F}, \vec{n} \times \vec{F})$ built from the matrix elements of the Pauli matrices

$$\langle z|\vec{\sigma}|z\rangle = -\vec{n}, \quad \text{and} \quad [z|\vec{\sigma}|z\rangle = i\vec{F} + \vec{n} \times \vec{F}. \qquad (3)$$

In the following, we will work with unit norm spinors $\langle z|z\rangle = 1$ to simplify the formulas if not specified otherwise.
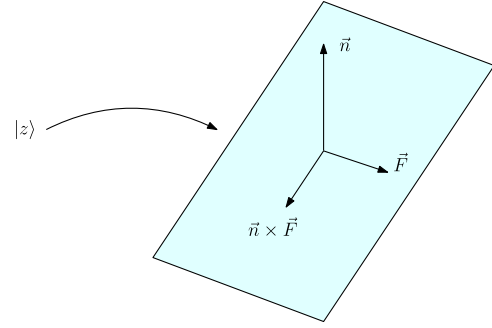

FIG. 1. Pictorial representation of the reference frame associated to a spinor $|z\rangle$. The magnitude of the spinor determines the plane and the phase of the spinor the frame of the plane.

In this case, the associated $\mathbb{R}^3$ basis is orthonormal. Each spinor identifies a (framed) plane in $\mathbb{R}^3$ orthogonal to $\vec{n}$ equipped with a frame given by the vector $\vec{F}$ (sometimes we will call it frame vector [19]). See Fig. 1 for a pictorial representation. Intuitively, the magnitude of the spinor determines the vector $\vec{n}$ while its phase (flag) characterizes completely the frame vector $\vec{F}$.

This geometrical interpretation is the same one used in the geometrical interpretation of loop quantum gravity states given by *twisted geometries* [18,24–26].

A general $SL(2, \mathbb{C})$ group element g can be parametrized by two (unit) spinors $|z\rangle$, $|w\rangle$ and a complex number ω,

$$g = e^{\frac{\omega}{2}}|w\rangle\langle z| + e^{-\frac{\omega}{2}}|w][z|. \qquad (4)$$

The group element g maps the source framed plane $|z\rangle$ into the target one $|w\rangle$. The complex angle ω encodes the boost angle and part of the rotation between the planes (see Appendix B for more details). The parametrization (4) is very redundant. Three real numbers parametrize each unit spinor (i.e., two angles to determine $\vec{n}$ and a third to determine $\vec{F}$ in the orthogonal plane). The complex number ω contributes to the count with two real degrees of freedom. The parametrization [4] is redundant. We use eight real parameters to specify a $SL(2, C)$ group element. Only six are necessary, and we can remove two safely. The parametrization [4] is invariant under the transformations

$$|z\rangle \to e^{i\alpha_1}|z\rangle \quad \text{and} \quad |w\rangle \to e^{i\alpha_1}|w\rangle,$$
$$|z\rangle \to e^{i\alpha_2}|z\rangle \quad \text{and} \quad \omega \to \omega - i\alpha_2, \qquad (5)$$

and equivalent combinations of the two. It is possible to remove two parameters among the phases of the spinors and Imω by reabsorbing it in the third using (5). In the following, we will work with the redundant parametrization since it has a simpler geometric interpretation. Notice, that also the dual group element $(g^{-1})^\dagger$ defines a map between the source and target frames $|z\rangle$, $|w\rangle$ with opposite chirality and can be obtained from (4) sending $\omega \to -\omega^*$.

The parametrization (4) is analog to the parametrization of the $SU(2)$ holonomy of the Ashtekar connection in *twisted geometries* [18,24–26] and can be recovered from (4) setting Re$\omega = 0$ and removing the redundant Imω. A form equivalent to (4) is derived in the context of covariant twisted geometries in terms of twistors in [20].

While the spinorial space carries a representation (the fundamental one) of $SL(2, \mathbb{C})$, the three-dimensional space $\mathbb{R}^3$ spanned by $(\vec{n}, \vec{F}, \vec{n} \times \vec{F})$ does not. If we want to interpret the action of the Lorentz group on $\mathbb{R}^3$ we have to embed it in a larger space where a representation is realized. The embedding is not unique, and the interpretation depends on this choice. Among many possibilities, the EPRL model and the study of general $SL(2, \mathbb{C})$ invariants [11] suggest one in terms of γ-simple bivectors. We represent a bivector with electric and magnetic part $\vec{E}$ and $\vec{B}$ with a complex vector given by $\Pi = \vec{E} + i\vec{B}$. In electromagnetism, it is known as the Riemann-Silberstein vector. If the electric and magnetic parts of the bivector are proportional $\vec{B} = \gamma\vec{E}$ we say the bivector is γ-simple (in the canonical frame). In this case we parametrize it with a complex number $j + i\gamma j$ and a unit vector $\vec{n}$. Or, in terms of the spinor $|z\rangle$,

$$\Pi = j(1 + i\gamma)\vec{n} = -j(1 + i\gamma)\langle z|\vec{\sigma}|z\rangle. \tag{6}$$

In the context of the EPRL spin foam model, we interpret j as quanta of areas and γ as the Immirzi parameter. This particular bivector is the consequence of constructing and implementing the linear simplicity constraints in the EPRL model. The bivector Π transform in the finite-dimensional representation of $SL(2, \mathbb{C})$ usually denoted as $(0, 1)$. Therefore, we can see a group element (4) as a map between the two γ-simple bivectors associated with $|z\rangle$ and $|w\rangle$[1]

$$\begin{aligned} g \triangleright \Pi &= j(1 + i\gamma)\langle z|g^{-1}\vec{\sigma}g|z\rangle \\ &= e^{\frac{-\omega+\omega}{2}}j(1 + i\gamma)\langle w|\vec{\sigma}|w\rangle = \Pi'. \end{aligned} \tag{7}$$

Since Π transforms in the $(0, 1)$ representation, we have to use fundamental representation and its dual. To make the bilinear (6) transform in the $(0, 1)$ representation we need both $|z\rangle$ and $\langle z|$ with the same chirality. This is the reason for the presence of the inverse group element (7).

Since we are interested in keeping the results as general as possible, we would not rely on this interpretation, so we will not specify any embedding until we talk about the EPRL model. We consider (4) as a map between spinors that only then do we interpret as framed planes. This is what

***

[1]Note that if we apply g to a γ-simple bivector, that is not the one associated to the source spinor of g the transformation is complicated and, in general, it will not be mapped into another γ-simple bivector.
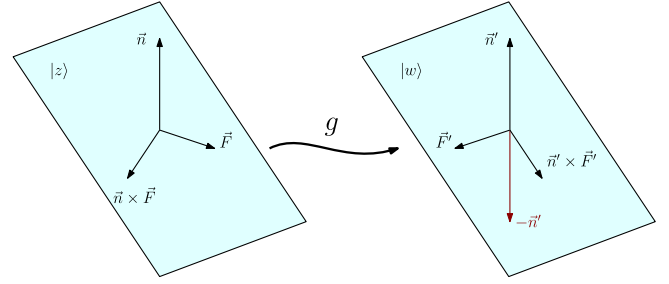

FIG. 2. Pictorial representation of the holonomy as a map between reference frames.

we mean, with a slight abuse of language, when we will say that (4) is a map between framed planes.

In the following, we shift the focus from general framed planes to planes representing the faces of framed polyhedra. With this goal in mind, it is convenient to use a holonomy that maps the framed plane $|z\rangle$ into the framed plane dual to $|w\rangle$

$$g = e^{\frac{\omega}{2}}|w]\langle z| - e^{-\frac{\omega}{2}}|w\rangle[z|. \tag{8}$$

In this way, the framed planes associated with the faces of polyhedra will have all outgoing normals. This is just a change of convention to ease the future geometrical interpretation. See Fig. 2 for a pictorial representation.

III. WEDGE HOLONOMIES AND LOCAL FLATNESS

We consider the 2-complex of a 4-simplex as illustrated in Fig. 3. It comprises five edges (dual to tetrahedra) and ten faces (dual to triangles). A face in a vertex is also called a wedge and contains two edges. We orient the wedges indicating the source and the target edge. We label each
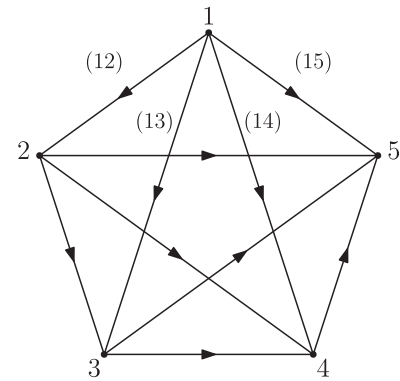

FIG. 3. The 2-complex of a 4-simplex. The edges are numbered from 1 to 5. A couple of edges label the wedges (faces in a vertex). To keep the picture clean, we just explicitly wrote the name of the wedges involving edge 1. We oriented the wedges ab with $a < b$ such that a is the source and b is the target of the wedge.

edge with an index $a = 1, \ldots, 5$ and each wedge with the couple ab where a is the source, and b is the target.

We associate a $SL(2, \mathbb{C})$ group element g_{ab} to every wedge (ab) representing the holonomy along that wedge. It describes the parallel transport from edge a to edge b. Following (8), we parametrize it as

$$g_{ab} = e^{\frac{\omega_{ab}}{2}} |z_{ba}] \langle z_{ab}| - e^{-\frac{\omega_{ab}}{2}} |z_{ba}\rangle [z_{ab}|. \qquad (9)$$

The spinor $|z_{ab}\rangle$ identifies a framed plane at the source edge a and the spinor $|z_{ba}\rangle$ identifies a framed plane at the target edge b. Given an edge a, four holonomies involve it, and four framed planes, identified by the spinors $|z_{ab}\rangle$ with $b \neq a$, are associated with it. With this notation, the inverse of (9) and the holonomy of the wedge with inverted orientation are related by $g_{ba} = -g_{ab}^{-1}$.

Spin foam models are *locally flat*; they are built using flat 4-simplices (or, more general, four-dimensional cells). In terms of holonomies, a 4-simplex is flat if the parallel transport along any cycle is trivial.[2] For example, for a 3-cycle (abc), the parallel transport is trivial if

$$g_{ca} g_{bc} g_{ab} = \mathbb{1}. \qquad (10)$$

For a simplicial vertex (as Fig. 3), imposing (10) on all the 3-cycles is sufficient to guarantee that the parallel transport on any cycle is trivial.[3] The generalization, to a general cell [9,10,27] is straightforward. However, we need to be careful to consider the correct number and order of cycles (higher-order cycles are probably necessary [10,28]).

A general set of holonomies is not *locally flat*. We impose it as a requirement. We find some constraints on the spinors and complex angles parametrizing the wedge holonomies (9). After some lengthy but straightforward algebra (that we report in detail in Appendix C), we find that Eq. (10) on every 3-cycle are equivalent to

$$\cosh(\omega_{ab} + i\xi_{ab}^c) = \cos \hat{\theta}_{ab}^c, \qquad (11)$$

for each wedge ab and

$$\sin \phi_{ac}^b \sinh(\omega_{ab} + i\xi_{ab}^c) = \sin \phi_{ab}^c \sinh(\omega_{ca} + i\xi_{ac}^b). \qquad (12)$$

for each couple of wedges ab and ac. The angles $\hat{\theta}_{ab}^c$ and ξ_{ab}^c are functions of the spinors and have an interesting geometrical interpretation.

The angle $\hat{\theta}_{ab}^c$ is the *generalized dihedral angle* and is given by the expression

$$\cos \hat{\theta}_{ab}^c = \frac{-|\langle z_{ca}|z_{cb}]|^2 + |\langle z_{ab}|z_{ac}\rangle|^2 |\langle z_{ba}|z_{bc}\rangle|^2 + |\langle z_{ac}|z_{ab}]|^2 |\langle z_{ba}|z_{bc}]|^2}{2|\langle z_{ac}|z_{ab}\rangle \langle z_{ac}|z_{ab}] \langle z_{ba}|z_{bc}\rangle \langle z_{ba}|z_{bc}]|} = \frac{\cos \phi_{ab}^c + \cos \phi_{cb}^a \cos \phi_{ac}^b}{\sin \phi_{cb}^a \sin \phi_{ac}^b}, \qquad (13)$$

where in the last equality we wrote the spinorial scalar products explicitly in terms of the 3D dihedral angles ϕ_{bc}^a between framed planes $|z_{ab}\rangle$ and $|z_{ac}\rangle$ (see Appendix A).

The readers familiar with 4D geometry will recognize in (13) the definition of the angle between the hyperplanes a and b when embedded in 4D, reconstructed using the spherical cosine laws. Without the hat, we will denote the geometric angle with θ_{ab}^c.[4] The spherical cosine laws have the same form for Euclidean and Lorentzian signatures of the embedding space. If $|\cos \hat{\theta}_{ab}^c| < 1$ it is Euclidean and if $|\cos \hat{\theta}_{ab}^c| > 1$ it is Lorentzian. In the first case, the angle is real and $\hat{\theta}_{ab}^c = \theta_{ab}^c$. In the last case, both hyperplanes are embedded as spacelike hyperplanes. The angle is imaginary and $i\theta_{ab}^c = \hat{\theta}_{ab}^c - \chi_{ab}\pi$ where $\chi_{ab} = 0$ $(\cos \hat{\theta}_{ab}^c > 1)$ for *cochronal* hyperplanes and $\chi_{ab} = 1$ $(\cos \hat{\theta}_{ab}^c < 1)$ for *antichronal* hyperplanes.

The generalized dihedral angle (13) depends only on absolute values of spinors scalar products. On the contrary, the *twist angle* ξ_{ab}^c depends explicitely on the phases of the spinors

$$\xi_{ab}^c = \arg\left(\frac{\langle z_{ac}|z_{ab}\rangle \langle z_{ab}|z_{ac}\rangle}{\langle z_{bc}|z_{ba}\rangle [z_{ba}|z_{bc}\rangle}\right). \qquad (14)$$

It is the edge-dependent and gauge-invariant twist angle studied extensively in the *twisted-geometry* literature [18,21,29–31]. It measures the twist between the frames of the planes ab and ba (source and target of the wedge ab) using ac and bc as a reference when parallel transported in the same frame with the Ashtekar holonomy. You can follow these steps if you want to visualize the twist angle. Consider the framed plane $|z_{ab}\rangle$ and its intersection with the framed plane $|z_{ac}\rangle$. Do the same with

---

[2]A cycle is a closed, ordered collection of wedges. For example $(abc) = \{(ab), (bc), (ca)\}$ is a 3-cycle. A cycle made of three wedges.

[3]All the cycles of a general graph are generated composing a the *fundamental cycles*. For a 4-simplex, the fundamental cycles are given by a set of six independent 3-cycles. We will consider all 3-cycles even if redundant to deal with symmetric equations.

[4]Please note the *plus* sign in the numerator of (13). At first glance, it seems to disagree with the analog formula reported in some literature [29]. The difference resides in the conventions that we use where *all* the dihedral angles (4D, 3D, 2D) are external. The factor π of difference compensates for the different sign. The inverse spherical cosine laws have the opposite sign.

$|z_{ba}\rangle$ and $|z_{bc}\rangle$. Rotate all the framed planes in the edge b such that the framed plane $|z_{ba}\rangle$ coincide with $|z_{ab}\rangle$ and the frames are aligned. The twist angle measures the angle between the intersections of the framed planes with $|z_{ac}\rangle$ and $|z_{bc}\rangle$, respectively.

The local flatness equations [(11) and (12)] constrain both the spinors and the complex angles of the wedge holonomies. First, we obtain the complex angles as a function of the spinors by inverting the trigonometric functions. Second, we realize that we have multiple expressions for the same complex angles (one for each 3-cycle the wedge holonomy belongs to). These multiple expressions are consistent if the spinors satisfy some extra conditions.

The set of equations has been studied in the context of the asymptotic analysis of the EPRL vertex amplitude. We summarize the result here and refer to [10] for a detailed analysis. We find two distinct classes of solutions.

The first one is characterized by $|\cos\hat{\theta}^c_{ab}| < 1$ for all cycles and the angles $\hat{\theta}^c_{ab} = \theta^c_{ab}$ are real. Inverting the trigonometric functions in (11) we find

$$\omega_{ab} = i\epsilon\theta^c_{ab} - i\xi^c_{ab}, \qquad (15)$$

were $\epsilon = \pm 1$ is a sign and has to be the same for all the wedges ab to satisfy (12). There are two ways to have the complex angle cycle independent. If the framed planes satisfy the *orientation conditions*[5] we can prove that $\theta^c_{ab} = \xi^c_{ab}$ for any c. Therefore, for $\epsilon = 1$ the complex angle is trivially cycle independent

$$\omega_{ab} = 0 \quad \forall \ ab \qquad (16)$$

is cycle independent. If $\epsilon = 1$, the combination $-\theta^c_{ab} - \xi^c_{ab}$ is not in general independent from the choice of c. However, if the spinors satisfy *angle-matching* conditions[6] the angles θ^c_{ab} and ξ^c_{ab} are individually independent form c (see [10,29,30,32] for an explicit proof). In this solution sector *angle-matching* conditions imply the *orientation conditions* as proved in [32]. In this case we drop the cycle dependent index c and the complex angles are purely imaginary and assume two possible values

$$\omega_{ab} = i\epsilon\theta_{ab} - i\xi_{ab}. \qquad (17)$$

---

[5]All the source and the target framed planes can be oriented in such a way their normals are pairwise opposite. The orientation can happen by rotating all the framed planes at the same edge with the same $SU(2)$ transformation. See [8] for complete geometric characterization.

[6]Consider the 2D angle α^{cd}_{ab} on the plane $|z_{ab}\rangle$ indentified by its intersection with the planes $|z_{ac}\rangle$ and $|z_{ad}\rangle$. Similarly, conder the corresponding 2D angle α^{cd}_{ba} identified by $|z_{ba}\rangle$, $|z_{bc}\rangle$, and $|z_{bd}\rangle$. The angle-matching condition is $\alpha^{cd}_{ab} = \alpha^{cd}_{ba}$ for all possible a, b, c, d.

In this case, we can imagine a 4D Euclidean embedding the edge hyperplanes and the angle θ_{ab} is the 4D dihedral angle between them in this embedding. The readers familiar with the spin foam literature are probably asking themselves where are vector geometries and the Euclidean 4-simplices. We will answer this question at the end of the section. In both cases the complex angles are vanishing or purely imaginary and the wedge holonomies are $SU(2)$ elements. Some parts of the literature refer to this as degenerate geometries. However, we prefer to call this class of solution the *topological sector* to highlight the $SU(2)$ nature of the holonomy. In fact, if we restrict the EPRL spin foam partition function to $SU(2)$ holonomies we obtain the partition function of the topological $SU(2)$ BF theory.

The second class of solutions is characterized by $|\cos\hat{\theta}^c_{ab}| > 1$ for all cycles. The angles $\hat{\theta}^c_{ab} = i\theta^c_{ab} + \chi_{ab}\pi$ are complex. Inverting the trigonometric functions in (11) we find

$$\omega_{ab} = \epsilon\theta^c_{ab} + i\chi^c_{ab}\pi - i\xi^c_{ab}. \qquad (18)$$

The sign $\epsilon = \pm 1$ is the same for all faces ab to satisfy (12). Since it is irrelevant, we dropped the sign from the term containing χ^c_{ab}. Because the angle is complex, the only way to have (18) independent from c is to have each of its terms independent from c. The *orientation conditions* cannot be satisfied. Once again, if the spinors satisfy *angle-matching* conditions the angles θ^c_{ab}, χ^c_{ab} and ξ^c_{ab} are independent from c [10,30,32]. In this case, we drop the cycle-dependent index c, and the complex angles assume two possible values

$$\omega_{ab} = \epsilon\theta_{ab} + i\chi_{ab}\pi - i\xi_{ab}. \qquad (19)$$

We embed the edge hyperplanes in a 4D Lorentzian space as spacelike hyperplanes. We call this sector of solutions the *Lorentzian sector*. The real part of the complex angle $\epsilon\theta_{ab}$ is the 4D dihedral angle between the hyperplanes a, b embedded in flat Lorentzian 4D space. The imaginary part has a causal term $\chi_{ab}\pi$ that tracks if the hyperplanes are cochronal or antichronal, and a term ξ_{ab} measuring the twist between the framed planes ab and ba. The wedge holonomy has a boost and rotation part and takes the form

$$g_{ab} = e^{\frac{\epsilon\theta_{ab}+i\chi_{ab}\pi-i\xi_{ab}}{2}}|z_{ba}]\langle z_{ab}| - e^{\frac{\epsilon\theta_{ab}+i\chi_{ab}\pi-i\xi_{ab}}{2}}|z_{ba}\rangle[z_{ab}|. \quad (20)$$

The solution with different signs $\epsilon = \pm 1$ are related by the transformation $g_{ab} \xrightarrow{\epsilon\to-\epsilon} (g^\dagger_{ab})^{-1}$. This duality is related by the symmetry of the local flatness equations (10). We obtain a set of equivalent equations if we transform all the holonomies into their inverse-conjugate transpose.

Some clarifications are in order. We were cautious in naming the geometries emerging from the local flatness conditions (10). In the spin foam literature the geometries in the *topological sector* called *vector geometries*, *Euclidean*

4-simplices and the geometries in the *Lorentzian sector* are *Lorentzian 4-simplices*. If we impose only *local flatness* we are missing a crucial ingredient to do the same. We do not know if the framed planes at the edges form a tetrahedron. This can be done by adding a closure condition to each edge.

First, we associate each edge with an area. In the EPRL spin foam model, this area is quantized and given by a spin $j_{ab} = j_{ba}$. We will use the same name for coherence. For each edge a we impose a closure constraint on the spinors at that edge

$$\sum_{b \neq a} j_{ab} \langle z_{ab} | \vec{\sigma} | z_{ab} \rangle = 0. \qquad (21)$$

With this additional condition the framed planes at each edge a close forming a framed tetrahedron [33] with areas given by j_{ab}. If the tetrahedra exist, then the geometries in the topological sector satisfying the orientation conditions are vector geometries. The angle-matching condition is equivalent to proper shape-matching conditions since the areas of corresponding triangles match by construction. The geometries in the topological sector satisfying the shape-matching conditions form a Euclidean 4-simplex. The geometries in the Lorentzian sector satisfying the shape-matching conditions form a Lorentzian 4-simplex. The closure conditions (21) are defined up to a global rescaling of all the areas $j_{ab} \to \lambda j_{ab}$. Therefore, the geometries we reconstruct are defined up to a global scale.

IV. THE EPRL MODEL AND LOCAL FLATNESS

The EPRL spin foam transition amplitude on a given simplicial 2-complex Δ with faces colored by $SU(2)$ spins j_f and edges colored by intertwiners i_e is given by

$$A_\Delta = \sum_{j_f, i_e} \prod_f A_f \prod_e A_e \prod_v A_v. \qquad (22)$$

The face amplitude is given by $A_f = 2j_f + 1$ and the edge amplitude by $A_e = 2i_e + 1$. They are fixed [34] requiring the correct convolution property of the path integral with a fixed boundary. The simplicial EPRL vertex amplitude A_v in the spinorial basis is formulated associating to each wedge ab a spin j_{ab} and the function

$$D^{(\gamma j_{ab}, j_{ab})}_{j_{ab} \mathcal{J} \zeta_{ba} j_{ab} \zeta_{ab}}(g_{ab}), \qquad (23)$$

where g_{ab} is the wedge holonomy, $D^{(\gamma j_{ab}, j_{ab})}_{j_{ab} \mathcal{J} \zeta_{ba} j_{ab} \zeta_{ab}}$ is a γ-simple unitary irreducible representation of $SL(2, \mathbb{C})$, and γ is the Immirzi parameter. The choice of the particular γ-simple representation is due to the weak quantum implementation of the linear simplicity constraints. Classically, it is responsible for reducing the Lorentzian topological BF theory to general relativity. In the spinorial basis, the γ-simple irrep (23) can be written in exponential form using a dummy spinor w_{ab} necessary to implement the unitarity of the representation

$$D^{(\gamma j_{ab}, j_{ab})}_{j_{ab} \mathcal{J} \zeta_{ba} j_{ab} \zeta_{ab}}(g_{ab}) = \frac{2j_{ab}+1}{\pi} \int dw_{ab} \frac{[\zeta_{ba}|w_{ab}\rangle^{2j_{ab}} \langle w_{ab}|g_{ab}|\zeta_{ab}\rangle^{2j_{ab}}}{\|w_{ab}\|^{2j_{ab}+2i\gamma j_{ab}+2} \|g^\dagger_{ab} w_{ab}\|^{2j_{ab}-2i\gamma j_{ab}+2}} = \int dw_{ab} \mu_{ab} e^{S_{ab}}, \qquad (24)$$

where the function $\mu_{ab} = \frac{2j_{ab}+1}{\pi} \frac{1}{\|w_{ab}\|^2 \|g^\dagger_{ab} w_{ab}\|^2}$ is usually interpreted as a measure factor. The wedge action is

$$S_{ab} = 2j_{ab} \log\left(\frac{[\zeta_{ba}|w_{ab}\rangle \langle w_{ab}|g_{ab}|\zeta_{ab}\rangle}{\|w_{ab}\|^{1+i\gamma} \|g^\dagger_{ab} w_{ab}\|^{1-i\gamma}} \right). \qquad (25)$$

The vertex amplitude A_v is constructed taking the product of (23) on all the wedges. Then, assigning a holonomy to each edge g_a such that $g_{ab} = g_b^{-1} g_a$. And finally, integrating over the edge holonomies, being careful to remove a redundant integration to regularize the amplitude [35],

$$A_v = \int \prod_a dg_a \delta(g_1) \prod_{ab} D^{(\gamma j_{ab}, j_{ab})}_{j_{ab} \mathcal{J} \zeta_{ba} j_{ab} \zeta_{ab}}(g_b^{-1} g_a). \qquad (26)$$

The model is usually introduced in this way, and the literature rarely comments on the choice of assigning holonomies to edges. Introducing the edge holonomy g_a related to the wedge holonomy via $g_{ab} = g_b^{-1} g_a$ implements

the *local flatness* condition strongly in the EPRL model. Local flatness is not a requirement of the discretization prescription we use in formulating the EPRL model. It is an ingredient we add to the mix because we want to work with flat simplices. To highlight it, we rewrite the vertex amplitude (26) using all ten wedge holonomies and imposing *local flatness* strongly with a delta function for each fundamental cycle of the 4-simplex.

$$A_v = \int \left(\prod_{ab} dg_{ab} D^{(\gamma j_{ab}, j_{ab})}_{j_{ab} \mathcal{J} \zeta_{ba} j_{ab} \zeta_{ab}}(g_{ab}) \right) \mathcal{C}_{LF}(g_{ab}, \ldots, g_{cd}) \quad (27)$$

An explicit example of $\mathcal{C}_{LF}$ based on a choice of fundamental cycles is

$$\mathcal{C}_{LF}(g_{ab}, \ldots, g_{cd}) = \delta(g_{13}^{-1} g_{23} g_{12}) \delta(g_{14}^{-1} g_{24} g_{12}) \delta(g_{15}^{-1} g_{25} g_{12})$$
$$\times \delta(g_{14}^{-1} g_{34} g_{13}) \delta(g_{15}^{-1} g_{35} g_{13}) \delta(g_{15}^{-1} g_{45} g_{14}). \qquad (28)$$

An explicit integration shows that we can eliminate six wedge holonomies g_{ab} with $a > 1$ from (27) out of ten. We obtain exactly the formula of the amplitude (26) if we identify the edge holonomies g_b with g_{1b}. Different choices of fundamental cycles in (28) correspond to different regularizations of (26) where a different redundant edge integration is removed.

V. THE LARGE SPIN LIMIT OF THE EPRL VERTEX AMPLITUDE

In the large spin regime, we consider the spins associated with the faces EPRL vertex amplitude homogenously large

$$j_{ab} \to \lambda j_{ab} \quad \text{with} \quad \lambda \gg 1. \tag{29}$$

We will refer to λ as the scale of the spins. We recast the vertex amplitude in exponential form using (24) with a total action

$$S = \sum_{ab} S_{ab} = \sum_{ab} 2 j_{ab} \log\left(\frac{[\zeta_{ba}|w_{ab}\rangle\langle w_{ab}|g_{ab}|\zeta_{ab}\rangle}{\|w_{ab}\|^{1+i\gamma}\|g_{ab}^\dagger w_{ab}\|^{1-i\gamma}}\right). \tag{30}$$

The action (30) is linear in the spins. Therefore, we can approximate the vertex amplitude using saddle-point techniques. The saddle points dominate the integrals of the vertex amplitude and are the points where the gradient of the action vanishes. Among them, we focus on those maximizing the real part of the action and giving the dominant contributions to the asymptotic behavior of the vertex amplitude. The real part of the wedge actions is negative $\mathrm{Re}S_{ab} \le 0$. The maximum of the real part of whole action (30) is obtained when $\mathrm{Re}S_{ab} = 0$ for all wedges. Strictly speaking, we should consider all the saddle points. Traditionally, the dominant ones are studied since the additional equations simplify the calculations. It would be interesting to study what changes if we relax the dominance request, especially in extended triangulations [22,36,37]. The saddle-point equations are

$$\frac{\delta S}{\delta g_a} = 0 \tag{31}$$

$$\frac{\delta S}{\delta w_{ab}} = 0 \tag{32}$$

$$\frac{\delta S}{\delta \bar{w}_{ab}} = 0 \tag{33}$$

$$\mathrm{Re}S_{ab} = 0 \tag{34}$$

We combine the saddle point equations to recast them in a form with a simpler geometrical interpretation. From (31) using the other equations to remove the dummy spinors w_{ab}, we obtain the closure condition for the boundary spinors

$$\sum_{b \ne a} j_{ab}\langle\zeta_{ab}|\vec{\sigma}|\zeta_{ab}\rangle = 0. \tag{35}$$

As we already discussed in (21) this condition allows interpreting the boundary framed planes as framed tetrahedra with areas given by the spins j_{ab}.

Combining the other three equations [(34), (32) and (33)] we obtain some equations that can be used to determine the value of the dummy spinors at the saddle point (we will not report them since they are not important for our discussion) and the equations that constrain the wedge holonomies' spinors in terms of the boundary ones. We use wedge holonomies to separate the saddle-point equations from the local flatness equation g_{ab} instead of the edge holonomies.

$$g_{ab}|\zeta_{ab}\rangle = \lambda_{ab}|\zeta_{ba}], \qquad (g_{ab}^{-1})^\dagger|\zeta_{ab}\rangle = \frac{1}{\lambda_{ab}^*}|\zeta_{ba}], \tag{36}$$

where the proportionality parameter λ_{ab} is to be determined. We have one alignment equation for each wedge ab fixing the parameters of the wedge holonomies (9) in terms of the boundary states.

$$g_{ab} = e^{\frac{\omega_{ab}}{2}}|\zeta_{ba}]\langle\zeta_{ab}| - e^{-\frac{\omega_{ab}}{2}}|\zeta_{ba}\rangle[\zeta_{ab}|, \tag{37}$$

where the porportionality coefficient is related to the complex angle $\lambda_{ab} = e^{\frac{\omega_{ab}}{2}}$ and still free.[7]

On shell of the alignment equations (36) the action (30) assumes a very simple form in terms of the complex angles ω_{ab}

$$S^{(cr)} = \sum_{ab} S_{ab}^{(cr)} = i\lambda \sum_{ab} j_{ab}(\gamma\mathrm{Re}\omega_{ab} + \mathrm{Im}\omega_{ab}). \tag{38}$$

Suppose we do not impose the local flatness conditions. In that case, the complex angles in (37) are undetermined, and the closure conditions (21) are the only restrictions on the boundary spinors. To connect with discrete 4D geometries and reproduce the famous result for which Lorentzian Regge action (and geometry) emerge in the semiclassical limit of the EPRL vertex amplitude, we have to include the local flatness conditions that we discussed in great length in Sec. III. They require additional constraints on the spinors and fix the complex angles in terms of the holonomies' spinors. For example, if we restrict to the Lorentzian sector, local flatness requires the framed tetrahedra described by the boundary spinors to satisfy the shape-matching constraints. We can reconstruct a Lorentzian 4-simplex with a spacelike boundary embedding the framed tetrahedra in 4D. The real part of the complex angles equals the dihedral angles. The imaginary part of the complex angles relates to

---

[7]The proof is straightforward. We write g_{ab} in terms of the four bilinears $|\zeta_{ba}\rangle\langle\zeta_{ab}|, |\zeta_{ba}\rangle\langle\zeta_{ab}|, |\zeta_{ba}\rangle[\zeta_{ab}|, |\zeta_{ba}][\zeta_{ab}|$ that form a basis of $GL(2,\mathbb{C})$ and we use (36) and $\det g_{ab} = 1$ to determine the complex coefficients.

the twist angle between the two framed tetrahedra. The action at the saddle point in this case becomes

$$S^{(cr)} = i\lambda\epsilon\sum_{ab}\gamma j_{ab}\theta_{ab} - i\lambda\sum_{ab}j_{ab}\xi_{ab} + i\lambda\epsilon\pi\sum_{ab}j_{ab}\chi_{ab}$$
$$= i\lambda\epsilon S_R - i\lambda T + i\lambda\epsilon\pi\Upsilon. \tag{39}$$

The first term is the well known Regge action of the 4-simplex $S_R = \sum_{ab}\gamma j_{ab}\theta_{ab}$ with areas γj_{ab} and Lorentzian dihedral angles θ_{ab}. The sign ϵ, which labels the two solutions of the local flatness equations, represents the two possible orientations of the 4-simplex with given boundary spacelike tetrahedra. The second term $T = \sum_{ab}j_{ab}\xi_{ab}$ is a twist term describing how the holonomies transform the frames of the boundary triangles. The last term $\Upsilon = \sum_{ab}j_{ab}\chi_{ab}$ is related to the "causal" structure of the 4-simplex and encodes the cochronality or antichronality of the boundary tetrahedra in the 4-simplex.

The effect of the local flatness condition on the Hessian of the saddle point expansion in the EPRL model is still unknown in closed form. It can be computed numerically [12], and its mathematical properties are known [38]. In particular, the Hessian is nondegenerate for geometries corresponding to nondegenerate 4-simplices. It could be interesting to study the nondegeneracy of the Hessian off shell of the local flatness condition and how they contribute. We leave this challenging calculation to future work.

VI. EXTENDED EPRL SPIN FOAM AMPLITUDES

The next step is considering spin foam amplitudes with more than a vertex. Before discussing the amplitude of the EPRL model specifically, we will make some general observations. For simplicity of notation, let us consider the most straightforward case of two vertices glued together on two edges. The 2-complex associated with this amplitude has two bulk edges and a bulk face (see Fig. 4 for reference). We decorate with tides the variables associated
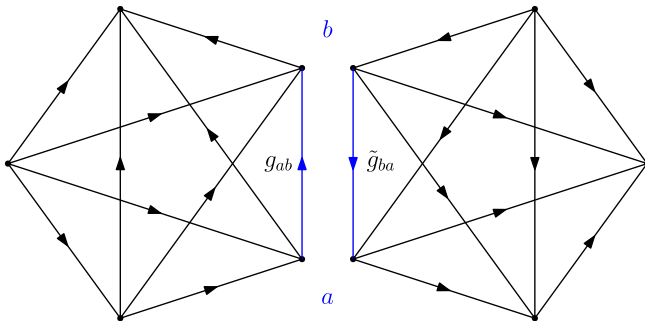

FIG. 4. Two spin foam vertices glued together. We denoted with a and b the bulk edges (highlighted in blue). The bulk face (also highlighted in blue) connects the two vertices and comprises the two wedges (one for each vertex) that include the bulk edges. We indicate the two bulk holonomies with g_{ab} and $\tilde{g}_{ba}$.

with the second vertex and look at the holonomies related to the bulk face. Using the parametrization (9) the two bulk holonomies are

$$g_{ab} = e^{\frac{\omega_{ab}}{2}}|z_{ba}\rangle\langle z_{ab}| - e^{-\frac{\omega_{ab}}{2}}|z_{ba}\rangle[z_{ab}|, \quad \text{and}$$
$$\tilde{g}_{ba} = e^{\frac{\tilde{\omega}_{ba}}{2}}|\tilde{z}_{ab}\rangle\langle \tilde{z}_{ba}| - e^{-\frac{\tilde{\omega}_{ba}}{2}}|\tilde{z}_{ab}\rangle[\tilde{z}_{ba}|. \tag{40}$$

In general, the two holonomies in their (9) form do not glue nicely. The framed plane $|z_{ba}\rangle$ of g_{ab} is independent from the framed plane $|\tilde{z}_{ba}\rangle$ of $\tilde{g}_{ba}$. The details of how the two holonomies glue is given by the details of the spin foam theory.

We focus on the contribution to the EPRL spin foam amplitude A_Δ (22) deriving from the bulk face. Each vertex contributes with a γ-simple unitary irreducible representation (23)

$$D^{(\gamma j_{ab}, j_{ab})}_{j_{ab}\mathcal{J}\zeta_{ba}j_{ab}\zeta_{ab}}(g_{ab}), \quad \text{and} \quad D^{(\gamma j_{ab}, j_{ab})}_{j_{ab}\mathcal{J}\tilde{\zeta}_{ab}j_{ab}\tilde{\zeta}_{ba}}(\tilde{g}_{ba}). \tag{41}$$

We glue the two vertices together with the factors $\langle\zeta_{ab}|\tilde{\zeta}_{ab}]^{2j_{ab}}$ and $\langle\zeta_{ba}|\tilde{\zeta}_{ba}]^{2j_{ab}}$ due to the fact that the spinorial basis is overcomplete. We integrate over the four spinors ζ with the appropriate measure.[8] If we put (41) in the exponential form we find that the face contributes to the amplitude with an action

$$S_f = 2j_{ab}\log\left(\frac{[\zeta_{ba}|w_{ab}\rangle\langle w_{ab}|g_{ab}|\zeta_{ab}\rangle}{\|w_{ab}\|^{1+i\gamma}\|g^\dagger_{ab}w_{ab}\|^{1-i\gamma}}\right) + 2j_{ab}\log\langle\zeta_{ab}|\tilde{\zeta}_{ab}]$$
$$+ 2j_{ab}\log\left(\frac{[\tilde{\zeta}_{ab}|\tilde{w}_{ab}\rangle\langle\tilde{w}_{ab}|\tilde{g}_{ba}|\tilde{\zeta}_{ba}\rangle}{\|\tilde{w}_{ab}\|^{1+i\gamma}\|\tilde{g}^\dagger_{ab}\tilde{w}_{ab}\|^{1-i\gamma}}\right)$$
$$+ 2j_{ab}\log\langle\tilde{\zeta}_{ba}|\zeta_{ba}]. \tag{42}$$

All the spinors in (42) are bulk spinors used to glue the vertices or dummy spinors used i nthe $SL(2,\mathbb{C})$ representations. We are integrating over all of them.

The whole EPRL amplitude (22) is defined with a sum over spins associated with bulk faces. Before considering the effect of the sum, we analyze the amplitude for a fixed value of the bulk face spin.

The action (42) is still linear in the spins j_{ab} and in the large spins regime (29) we can approximate the spin foam amplitude using saddle point techniques. The saddle point is made on all the variables. Now they also include bulk spinors. Again we look for the dominant saddle points where the gradient of the action vanishes, and the real part of the action is maximal. Since $\mathrm{Re}S \leq 0$ and both the contribution coming from the vertices and the gluing are negative and at most zero, maximizing $\mathrm{Re}S$ is equivalent to asking that the real part of each of its constituents (each logarithm) vanish independently.

---

[8]The integration measure is $d\zeta = 1/\pi i d^4\zeta$.

In addition to the saddle point equations we discussed in Sec. V for each vertex, the extra integrals over the bulk spinors lead to some additional equations

$$\frac{\delta S}{\delta \zeta_{ab}} = 0, \tag{43}$$

$$\frac{\delta S}{\delta \tilde{\zeta}_{ab}} = 0, \tag{44}$$

$$\text{Re} \log \langle \zeta_{ab} | \tilde{\zeta}_{ab}] = 0. \tag{45}$$

It has been shown with an explicit calculation [36,37] that on shell of the other critical-point equations (43) and (44) are automatically satisfied. The solution of Eq. (45) are simple and requires the bulk edge spinors to coincide up to a phase

$$|\zeta_{ab}\rangle = e^{-i\alpha_{ab}}|\tilde{\zeta}_{ab}], \quad \text{and} \quad |\zeta_{ba}\rangle = e^{-i\alpha_{ba}}|\tilde{\zeta}_{ba}]. \tag{46}$$

The saddle point analysis is identical to the single vertex case with the extra wedge gluing condition on bulk edge spinors. The action of the closed face (42) at the critical points is

$$S_f^{(cr)} = i\lambda j_{ab}(\gamma \text{Re}\omega_{ab} + \text{Im}\omega_{ab}) + i\lambda j_{ab}(\gamma \text{Re}\tilde{\omega}_{ab} + \text{Im}\tilde{\omega}_{ab}) + i2\lambda j_{ab}(\alpha_{ab} + \alpha_{ba}). \tag{47}$$

To make contact with geometry, we go on shell of each vertex's local flatness equations (10). If we restrict for brevity to a global Lorentzian sector,[9] the action of the closed face (42) reduces to

$$S_f^{(cr)} = i\lambda\gamma j_{ab}(\epsilon\theta_{ab} + \tilde{\epsilon}\tilde{\theta}_{ba}) - i\lambda j_{ab}(\xi_{ab} + \tilde{\xi}_{ba}) + i2\lambda j_{ab}(\alpha_{ab} + \alpha_{ba}) + i\lambda\pi j_{ab}(\epsilon\chi_{ab} + \tilde{\epsilon}\tilde{\chi}_{ba}). \tag{48}$$

Recall that we decorate with a tilde the variables of the second vertex. The first term is the algebraic sum of the Lorentzian dihedral angle dual to the triangle (ab). It is related to the deficit angle associated with the triangle, and the relative sign $\epsilon/\tilde{\epsilon}$ is associated with the relative orientation of the two 4-simplices. The relative orientation of the two vertices is not fixed. If this is a desired feature of the EPRL model or if we want to remove it is not clear; however, the same freedom is present in the Ponzano-Regge model [39,40] where it is necessary to have a topological invariant model.

The last term is a sign for the amplitude, keeping track of the local causal structures of the two 4-simplices. The twist

---

[9]While critical-point equations (the spherical sine laws, to be precise) force all the holonomies in the same vertex to be in the same sector, there are no equations that require holonomies in different vertices to be in the same sector.

term combines with the overlapping term in an interesting way. Observe that, up to irrelevant factors of 2π, and using the conditions (46) for the closed face and the auxiliary face used to define the twist angles, we can express the sum of the twist angles as

$$\begin{aligned} \xi_{ab} + \tilde{\xi}_{ab} &= \arg\left(\frac{\langle\zeta_{ac}|\zeta_{ab}]\langle\zeta_{ab}|\zeta_{ac}\rangle}{\langle\zeta_{bc}|\zeta_{ba}\rangle[\zeta_{ba}|\zeta_{bc}\rangle}\right) \\ &+ \arg\left(\frac{\langle\zeta_{bc}|\zeta_{ba}\rangle[\zeta_{ba}|\zeta_{bc}\rangle}{\langle\zeta_{ac}|\zeta_{ab}]\langle\zeta_{ab}|\zeta_{ac}\rangle}\right) + 2(\alpha_{ab} + \alpha_{ba}) \\ &= 2(\alpha_{ab} + \alpha_{ba}), \end{aligned} \tag{49}$$

where the two arg functions cancel since their arguments are reciprocal. The twist contribution of the action summed with the overlap on shell vanish. The action of the closed face (42) restricted to a global Lorentzian sector reduces to a term proportional to the deficit angle and a "sign" term related to the Lorentzian structure of the two 4-simplices

$$S_f^{(cr)} = i\lambda\gamma j_{ab}(\epsilon\theta_{ab} + \tilde{\epsilon}\tilde{\theta}_{ba}) + i\lambda\pi j_{ab}(\epsilon\chi_{ab} + \tilde{\epsilon}\tilde{\chi}_{ba}). \tag{50}$$

It is interesting to also look at the form of the face holonomy on shell of the critical-point equations. Using the gluing equations (46) we have

$$g_f = \tilde{g}_{ba}g_{ab} = e^{\frac{\omega_{ab}+\tilde{\omega}_{ba}}{2}+i(\alpha_{ab}+\alpha_{ba})}|\zeta_{ab}\rangle\langle\zeta_{ab}| + e^{-\frac{\omega_{ab}+\tilde{\omega}_{ab}}{2}-i(\alpha_{ab}+\alpha_{ba})}|\zeta_{ab}][\zeta_{ab}|. \tag{51}$$

The holonomy g_f maps the framed plane $|z_{ab}\rangle$ to itself with a complex angle $\omega_f = \omega_{ab} + \tilde{\omega}_{ab} + i2(\alpha_{ab} + \alpha_{ba})$. The spinor $|\zeta_{ab}\rangle$ is constrained only by closure equations. In particular, g_f is a 4-screw, a composition of a boost of angle $\text{Re}\omega_f$ and a rotation of angle $\text{Im}\omega_f$ along the same axis $\vec{n}_{ab}$.

If we include the local flatness equations (10) and restrict ourselves to the global Lorentzian sector, we can furthermore simplify the expression for the complex angle ω_f

$$\omega_f = \gamma(\epsilon\theta_{ab} + \tilde{\epsilon}\tilde{\theta}_{ba}) + i\pi(\epsilon\chi_{ab} + \tilde{\epsilon}\tilde{\chi}_{ba}), \tag{52}$$

where we used (49) to cancel the twist angles with the gluing phases, in this sector, the face holonomy has the form of a Regge holonomy. It is a pure boost in the plane orthogonal to the triangle of an angle equal to the sum of the 4D dihedral angles dual to the triangles of the (two) 4-simplices that share it.

VII. THE SUM OVER THE SPINS

In the previous section we studied the large spins approximation of the spin foam amplitude with fixed bulk spins. The full spin foam amplitude (22) is obtained by weighting the contributions with a face amplitude $A_f = 2j_f + 1$ and summing over the spins associated with

bulk faces. To keep the notation simple, we will continue using the example introduced in the previous section. The generalization to arbitrary bulk faces immediately follows with the same reasoning and steps. Summing over its spin explicitly, the bulk face (ab) contributes to the spin foam amplitude with

$$
F_{\text{EPRL}}(g_{ab}, \tilde{g}_{ba}) = \sum_{j_{ab}} (2j_{ab}+1) \int (2j_{ab}+1) \mathrm{d}\zeta_{ab} \int (2j_{ab}+1) \mathrm{d}\zeta_{ba} \int (2j_{ab}+1) \mathrm{d}\tilde{\zeta}_{ab} \int (2j_{ab}+1) \mathrm{d}\tilde{\zeta}_{ba}
$$
$$
\times D^{(\gamma j_{ab}, j_{ab})}_{j_{ab} \mathcal{J}\zeta_{ba} j_{ab}\zeta_{ab}}(g_{ab}) \langle \zeta_{ab} | \tilde{\zeta}_{ab}]^{2j_{ab}} D^{(\gamma j_{ab}, j_{ab})}_{j_{ab} \mathcal{J}\tilde{\zeta}_{ab} j_{ab}\tilde{\zeta}_{ba}}(\tilde{g}_{ba}) \langle \tilde{\zeta}_{ba} | \zeta_{ba}]^{2j_{ab}}, \tag{53}
$$

where $\mathrm{d}\zeta$ is the measure over the spinor space. Notice that the integrals over the spinors could be performed exactly. We opt not to do it to use the same notation of the previous sections.

The partition function of the EPRL spin foam model can be rewritten as the product of functions like (53) associated with each face, a local flatness constraint for each vertex, and the integration over all the wedge holonomies. The equivalent of (53) for the BF topological spin foam theory is a group delta function of the product of the wedge holonomies associated with the face. In that case, the delta functions impose the global flatness of the model on the 2-complex, forcing any parallel transport to be trivial. A similar result for the EPRL model can be obtained by studying the wavefront set of the partition function. Studying it is a very involved process and has been proposed in the context of the Euclidean EPRL model in [23]. The analysis in [23] focuses more on mathematical rigor than its interpretation and uses a parametrization with numerous auxiliary variables. For these reasons, it remains an amazing paper not fully digested by the community. The takeaway message of their work we need for this section is that the singular support of the integrand dominates the integrals in the EPRL partition functions. The singular support of a distributions is essentially given by the group elements for which the distribution is singular (e.g. the singular support of $\delta(g_f)$ is given by $\text{Sing}(\delta) = \{\mathbb{1}\}$).

The calculation is lengthy but simple. We report it with all the details in Appendix D. The singular support of the function (53) is given by

$$
\text{Sing}(F_{\text{EPRL}}(g_{ab}, \tilde{g}_{ba})) = \{g_{ab}, \tilde{g}_{ba} | \tilde{g}_{ba} g_{ab}
$$
$$
= e^{\frac{\omega_f}{2}} |\zeta\rangle\langle\zeta| + e^{-\frac{\omega_f}{2}} |\zeta][\zeta| \text{ with } \gamma \text{Re}\omega_f
$$
$$
+ \text{Im}\omega_f = 0 \mod 4\pi\}. \tag{54}
$$

The singular support of (53) contains all the wedge holonomies such that their product (that forms the face holonomy representing the parallel transport around a bulk face) is a 4-screw. Its direction is arbitrary, and it has a rapidity and rotation angle proportional (the proportionality factor is $-\gamma$) up to 4π factors. Following the arguments of [23], we expect that such holonomies dominate the semiclassical limit. The result of the analog calculation for a face with an arbitrary number of vertices is the same.

The "naive" flatness problem [23,41–44] claims that, at fixed triangulation, the amplitude is dominated in the large (boundary) spin limit by flat geometries. For a path-integral formulation of a quantum theory, the amplitude is exponentially suppressed if and only if the boundary data is inconsistent with the classical equation of motions. Therefore, the flatness problem was interpreted as an indication that the EPRL model apparently cannot recover nonflat solutions of Einstein's equations. The problem disappears if the triangulation refinement is considered at the same time as the large spin limit.

However, we want to show that the same tension arises when we combine (54) with the large spin limit form of the face holonomy derived in the previous section (51) and local flatness conditions. In that case, the imaginary part of the complex angle of the face holonomy is the vanishing twist term. The real part of the complex angle is the sum of the dihedral angles associated with the bulk face. In this case, the singular support condition gives the (in)famous flatness equation $\gamma \sum_i \theta_i = 0 \mod 4\pi$.

The same conclusion can also be derived using saddle point techniques, and Poisson resummation [44]. We preferred to follow the singular support argument to demystify the result of [23] because it focuses more on the holonomies than the geometries.

VIII. DISCUSSION

We explored the implication of local flatness in Lorentzian spin foam models. We find that geometry emerges naturally from it, independently from the details of the models.

We associate a set of $SL(2, \mathbb{C})$ holonomies with the wedges of a spin foam vertex. We require the parallel transport within a simplicial spin foam vertex to be trivial and find constraints on the geometry that parametrize the holonomies. We parametrize each holonomy with two framed planes (one at the source and one at the target) and a complex angle representing the boost and twist between the planes. This interpretation is analog to the twisted-geometry picture of loop quantum gravity [18,20,21,30,31]. The local flatness equations impose conditions on the angles of the geometry that we divide into two classes. The first class of solutions contains $SU(2)$ holonomies. Moreover, the geometry has to satisfy

at least the orientation conditions, and the complex angles vanish. If the geometry satisfies angle-matching conditions, we can embed the 3D hyperplanes associated with the spin foam edges in Euclidean 4D space. The complex angles are related to the 4D dihedral angles and the twist between corresponding frames. The second class of solutions contains holonomies with a nontrivial boost part. The geometry satisfies angle-matching conditions, and we can embed the 3D hyperplanes associated with the spin foam edges as spacelike hyperplanes in a Lorentzian 4D space. The real part of the complex angles relates to the 4D dihedral angle between them, and the imaginary part to the twist between corresponding frames. If we require closure conditions of the framed planes associated with the same edge, we can interpret the framed planes as framed tetrahedra. If we supplement the local flatness condition with closure conditions, geometry in the topological sector reduces to a vector geometry or a Euclidean 4-simplex. Geometry in the Lorentzian sector reduces to a Lorentzian 4-simplex with a spacelike boundary. Closure conditions result from the theory's edge $SU(2)$ invariance. Assume we find a mechanism to select the Lorentzian sector of locally flat holonomies. Integrating over locally flat holonomies satisfying edge closure constraints restricted to the Lorentzian sector is equivalent to summing over all Lorentzian 4-simplices.

The correspondence between holonomies and Lorentzian geometry is model independent and very general. We do not have to mention semiclassical regimes, irreducible representations, or other ingredients necessary to build a model. The geometry of Lorentzian 4-simplices emerges naturally from the vertices of any locally flat Lorentzian spin foam theory with $SU(2)$ edge invariance. What role do the details of the spin foam model play? The model has to introduce a scale $\hbar$ that distinguishes the semiclassical regime from the quantum one. In the semiclassical regime, the model provides an action that tells us how to glue 4-simplices together and how to recover (discrete) Einstein equations. In the EPRL model, $\hbar$ multiplies the spins associated with the areas of the geometry. Therefore, we identify the semiclassical regime with the large quantum numbers regime.[10] We glue two 4-simplices together, identifying the shared tetrahedra up to the choice of frame. How to recover the Einstein equations in the theory is still unknown and is an object of active research. In this regime, the EPRL model also gives the edge closure conditions as saddle point equations and the action reduces to the area-angle Regge calculus area.

We believe this is the best starting point if we want to iterate and improve the EPRL spin foam model using a top-down approach starting from discrete general relativity. We

realize this is an arduous and lengthy path and that this work is only the first step in this direction.

We conclude with a few observations. The story we tell shows many connections with effective spin foams [45,46]. They abandon loop quantum gravity variables to work directly with flat Lorentzian 4-simplices, take the action of area-angle Regge calculus seriously, and study the gluing of 4-simplices with a term inspired by spin foams. In this work, we prove that the integral over $SL(2, \mathbb{C})$ holonomies of the EPRL model is somehow equivalent to the sum over Lorentzian 4-simplices of the effective model. We leave to future work, a more in-depth study on how to translate their results into the holonomies language that talks directly to traditional covariant loop quantum gravity.

There are numerous extensions of the EPRL model that includes 4-simplices with timelike boundary. Even if this work cannot apply directly to those models, local flatness is a fundamental ingredient also in that case. The parametrization (9) uses spinors that carry a representation of $SU(2)$, the subgroup of the Lorentz group stabilized by the normal of the spacelike hypersurface. We can repeat our analysis by changing the parametrization of the wedge holonomies with objects that carry a $SU(1, 1)$ representation. We expect to find comparable results in that case too.

APPENDIX A: ALGEBRA WITH SPINORS

Given a unit spinor $|z\rangle$ such that $\langle z|\vec{\sigma}|z\rangle = -\vec{n}$ we have that

$$|z\rangle\langle z| = \frac{\mathbb{1} - \vec{n} \cdot \vec{\sigma}}{2}, \qquad (A1)$$

is a projector on the one dimensional subspace of $\mathbb{C}^2$ spanned by $|z\rangle$. The orthogonal projector is given by

$$|z][z| = \frac{\mathbb{1} + \vec{n} \cdot \vec{\sigma}}{2}. \qquad (A2)$$

The sum of the two orthogonal projectors provides a resolution of the identity of $\mathbb{C}^2$

$$|z\rangle\langle z| + |z][z| = \mathbb{1}. \qquad (A3)$$

The scalar products of two unit spinors and their duals are related by the followind identities

---

[10]To be more precise, the community recently agreed upon identifying the semiclassical regime as a double limit of large quantum numbers and refined 2-complexes.

$$[z|w] = \langle w|z \rangle = \overline{\langle z|w \rangle}, \qquad [z|w \rangle = -[w|z \rangle = -\overline{\langle z|w]}. \quad (A4)$$

Therefore, a direct calculation shows that

$$|\langle w|z \rangle|^2 = 1 - |[w|z \rangle|^2. \qquad (A5)$$

Given two unit spinors $|z_{ab}\rangle$ and $|z_{ac}\rangle$ representing two framed planes we compute

$$|\langle z_{ab}|z_{ac}\rangle|^2 = \langle z_{ab}|z_{ac}\rangle\langle z_{ac}|z_{ab}\rangle = \langle z_{ab}|\frac{\mathbb{1} - \vec{n}_{ac}\cdot\vec{\sigma}}{2}|z_{ab}\rangle$$
$$= \frac{1 + \vec{n}_{ab}\cdot\vec{n}_{ac}}{2} = \frac{1 + \cos\phi_{bc}^a}{2}, \qquad (A6)$$

where $\cos\phi_{bc}^a = \vec{n}_{ab}\cdot\vec{n}_{ac}$ is the dihedral angle between the framed planes $|z_{ab}\rangle$ and $|z_{ac}\rangle$ orthogonal to $\vec{n}_{ab}$ and $\vec{n}_{ac}$. Using (A5) we have

$$|[z_{ab}|z_{ac}\rangle|^2 = \frac{1 - \cos\phi_{bc}^a}{2}. \qquad (A7)$$

Combining (A6) and (A7) and using basic trigonometry we also have

$$2|[z_{ab}|z_{ac}\rangle\langle z_{ab}|z_{ac}\rangle| = 2\sqrt{\frac{1 - \cos\phi_{bc}^a}{2}}\sqrt{\frac{1 + \cos\phi_{bc}^a}{2}}$$
$$= \sin\phi_{bc}^a, \qquad (A8)$$

where we assumed by convention that $0 \le \phi_{bc}^a \le \pi$.

APPENDIX B: CANONICAL FORM OF THE HOLONOMIES

Consider two spinors $|z\rangle$ and $|w\rangle$ representing the basis of two $\mathbb{C}^2$ spaces. If we interpret them as the source and target space of a linear map $g \in GL(2, \mathbb{C})$ we can parametrize it using the projectors and complex coefficients

$$g = a|w\rangle\langle z| + b|w]\langle z| + c|w\rangle[z| + d|w][z|. \quad (B1)$$

A general $g \in SU(2)$ element can be parametrized by

$$g = a|w\rangle\langle z| + b|w]\langle z| - b^*|w\rangle[z| + a^*|w][z|, \qquad (B2)$$

with the unit determinant condition $|a|^2 + |b|^2 = 1$. Moreover, we can always find a canonical basis for the source and target space for which

$$g = e^{i\frac{\phi}{2}}|w\rangle\langle z| + e^{-i\frac{\phi}{2}}|w][z|, \qquad (B3)$$

where the phase ϕ is redundant and can be reabsorbed in the phase of any of the two spinors. We keep it anyway since it is convenient for our analysis. We can also prove that

$$b = e^{\frac{\eta}{2}}|w\rangle\langle w| + e^{-\frac{\eta}{2}}|w][w|, \qquad (B4)$$

is an element of $SL(2, \mathbb{C})$ and is a pure boost. Using the projectors (A1) and (A2) and denoting with $\vec{m}$ the normal of the framed plane $|w\rangle$

$$b = e^{\frac{\eta}{2}}|w\rangle\langle w| + e^{-\frac{\eta}{2}}|w][w|$$
$$= \frac{e^{\frac{\eta}{2}} + e^{-\frac{\eta}{2}}}{2}\mathbb{1} - \frac{e^{\frac{\eta}{2}} - e^{-\frac{\eta}{2}}}{2}\vec{m}\cdot\vec{\sigma} = e^{-\eta\frac{\vec{m}\cdot\vec{\sigma}}{2}}, \qquad (B5)$$

which is the canonical form of a pure boost with rapidity η and axis $-\vec{m}$. It is clear, for arbitrary $\vec{m}$ ($|w\rangle$) and rapidity η we obtain all the possible boosts. The canonical form (4) can be decomposed in a pure boost times an arbitrary rotation. Therefore, it represent the most general Lorentz transformation $g \in SL(2, \mathbb{C})$

$$g = (e^{\frac{\text{Re}\omega}{2}}|w\rangle\langle w| + e^{-\frac{\text{Re}\omega}{2}}|w][w|)(e^{\frac{i\text{Im}\omega}{2}}|w\rangle\langle z| + e^{-\frac{i\text{Im}\omega}{2}}|w][z|). \qquad (B6)$$

APPENDIX C: SPHERICAL COSINE LAWS AND LOCAL FLATNESS

This section derives the spherical cosine and sine laws from the local flatness conditions. The calculation is straightforward, although lengthy. We start from the local flatness condition (10) where we isolate the wedge holonomy g_{ab}

$$g_{ab}^{-1} = g_{ca}g_{bc}. \qquad (C1)$$

It is more convenient to work with scalar equations than matricial ones. We take the matrix elements

$$[z_{ac}|g_{ab}^{-1}|z_{bc}\rangle = [z_{ac}|g_{ca}g_{bc}|z_{bc}\rangle,$$
$$\langle z_{ac}|g_{ab}^{-1}|z_{bc}] = \langle z_{ac}|g_{ca}g_{bc}|z_{bc}], \qquad (C2)$$

with the intent of isolating the complex angle ω_{ab}.[11] Substituting the explicit form of the wedge holonomies (9) we get

$$e^{-\frac{\omega_{ab}}{2}}[z_{ac}|z_{ab}\rangle[z_{ba}|z_{bc}\rangle - e^{\frac{\omega_{ab}}{2}}[z_{ac}|z_{ab}]\langle z_{ba}|z_{bc}\rangle$$
$$= e^{\frac{\omega_{ca}+\omega_{bc}}{2}}\langle z_{ca}|z_{cb}],$$
$$e^{-\frac{\omega_{ab}}{2}}\langle z_{ac}|z_{ab}\rangle[z_{ba}|z_{bc}] - e^{\frac{\omega_{ab}}{2}}\langle z_{ac}|z_{ab}]\langle z_{ba}|z_{bc}]$$
$$= e^{-\frac{\omega_{ca}+\omega_{bc}}{2}}[z_{ca}|z_{cb}\rangle. \qquad (C3)$$

Taking the term-by-term product of these two equations, we can eliminate the complex angles ω_{ca}, ω_{bc} and obtain

---

[11]The alternative projection $\langle z_{ac}| \cdot |z_{bc}\rangle$ and $[z_{ac}| \cdot |z_{bc}]$ leads to the same result with an equivalent path.

$$e^{\omega_{ab}}[z_{ac}|z_{ab}]\langle z_{ba}|z_{bc}\rangle\langle z_{ac}|z_{ab}\rangle\langle z_{ba}|z_{bc}\rangle + e^{-\omega_{ab}}\langle z_{ac}|z_{ab}\rangle[z_{ba}|z_{bc}][z_{ac}|z_{ab}][z_{ba}|z_{bc}\rangle$$
$$- [z_{ac}|z_{ab}]\langle z_{ba}|z_{bc}\rangle\langle z_{ac}|z_{ab}\rangle[z_{ba}|z_{bc}] - [z_{ac}|z_{ab}\rangle[z_{ba}|z_{bc}]\langle z_{ac}|z_{ab}\rangle\langle z_{ba}|z_{bc}] = \langle z_{ca}|z_{cb}\rangle[z_{ca}|z_{cb}] \tag{C4}$$

To isolate the complex angle ω_{ab} it is convenient to manipulate the equality using the properties (A4) and the definition of the twist angle (14)

$$\cosh(\omega_{ab} + i\xi_{ab}^c) = \frac{-|\langle z_{ca}|z_{cb}\rangle|^2 + |\langle z_{ab}|z_{ac}\rangle|^2|\langle z_{ba}|z_{bc}\rangle|^2 + |\langle z_{ac}|z_{ab}\rangle|^2|\langle z_{ba}|z_{bc}\rangle|^2}{|\langle z_{ac}|z_{ab}\rangle\langle z_{ac}|z_{ab}]\langle z_{ba}|z_{bc}\rangle\langle z_{ba}|z_{bc}]|}. \tag{C5}$$

Using the formulas to relate the absolute values of the spinor scalar products to the dihedral angles between framed planes (A6), (A7) and (A8) we finally obtain (11)

$$\cosh(\omega_{ab} + i\xi_{ab}^c) = \frac{\cos\phi_{ab}^c + \cos\phi_{bc}^a\cos\phi_{ac}^b}{\sin\phi_{bc}^a\sin\phi_{ac}^b}. \tag{C6}$$

To find the equivalent equations for the complex angles ω_{ca} and ω_{bc} we repeat the calculation isolating g_{ca} and g_{bc} at the fist step (C1).

The derivation of (12) is more complicated but involves only basic algebra and the spinorial calculus properties we introduced in Appendix A.[12] We will sketch the main steps and omit the majority of the algebra. We start with a particular combination of projections of the matrical equation (C1)

$$[z_{ac}|g_{ab}^{-1}|z_{bc}\rangle\langle z_{ac}|g_{ab}^{-1}|z_{bc}\rangle = [z_{ac}|g_{ca}g_{bc}|z_{bc}\rangle\langle z_{ac}|g_{ca}g_{bc}|z_{bc}\rangle, \tag{C7}$$

$$\langle z_{ac}|g_{ab}^{-1}|z_{bc}][z_{ac}|g_{ab}^{-1}|z_{bc}] = \langle z_{ac}|g_{ca}g_{bc}|z_{bc}][z_{ac}|g_{ca}g_{bc}|z_{bc}]. \tag{C8}$$

Then we substitute the explicit expression for the wedge holonomies (9), we divide the first equation by $\langle z_{ba}|z_{bc}\rangle[z_{ba}|z_{bc}\rangle$, the second by $\langle z_{ba}|z_{bc}][z_{ba}|z_{bc}]$ and we subtract them. The result, after a few simplifications, is

$$e^{\omega_{ab}}\frac{\langle z_{ac}|z_{ab}\rangle[z_{ac}|z_{ab}\rangle}{[z_{ba}|z_{bc}\rangle\langle z_{bc}|z_{ba}\rangle} - e^{-\omega_{ab}}\frac{\overline{\langle z_{ac}|z_{ab}\rangle[z_{ac}|z_{ab}\rangle}}{\overline{[z_{ba}|z_{bc}\rangle\langle z_{bc}|z_{ba}\rangle}} = e^{\omega_{bc}}\frac{\langle z_{cb}|z_{ca}\rangle\langle z_{ca}|z_{cb}\rangle}{\langle z_{ba}|z_{bc}\rangle[z_{ba}|z_{bc}\rangle} - e^{-\omega_{bc}}\frac{\overline{\langle z_{cb}|z_{ca}\rangle\langle z_{ca}|z_{cb}\rangle}}{\overline{\langle z_{ba}|z_{bc}\rangle[z_{ba}|z_{bc}\rangle}}. \tag{C9}$$

If we extract the phases from the scalar product, we can recognize the twist angles and collect the remaining absolute value

$$2\sinh(\omega_{ab} + i\xi_{ab}^c)\frac{|\langle z_{ac}|z_{ab}\rangle\langle z_{ac}|z_{ab}\rangle|}{|\langle z_{ba}|z_{bc}][z_{bc}|z_{ba}\rangle|} = 2\sinh(\omega_{bc} + i\xi_{bc}^a)\frac{|\langle z_{cb}|z_{ca}\rangle\langle z_{ca}|z_{cb}\rangle|}{|\langle z_{ba}|z_{bc}\rangle[z_{ba}|z_{bc}\rangle|}. \tag{C10}$$

In terms of the dihedral angles between framed planes (A6), (A7) and (A8) we obtain directly (12)

$$\sinh(\omega_{ab} + i\xi_{ab}^c)\sin\phi_{bc}^a = \sinh(\omega_{bc} + i\xi_{bc}^a)\sin\phi_{ab}^c. \tag{C11}$$

If in (C7) we start from the product of the projections $[z_{ac}|\cdot|z_{bc}\rangle[z_{ac}|\cdot|z_{bc}]$ and the complementary one we obtain the analog equation relating the complex angles ω_{ab} and ω_{ca}.

---

[12]We suspect there is a more straightforward derivation of these equations.

APPENDIX D: SINGULAR SUPPORT OF F_{EPRL}

We start from the expression (53), and we explicit the form of the γ-simple unitary irreducible representations. We find

$$
F_{EPRL}(g_{ab}, \tilde{g}_{ba}) = \sum_{j_{ab}} (2j_{ab} + 1) \int (2j_{ab} + 1) \mathrm{d}\zeta_{ab} \int (2j_{ab} + 1) \mathrm{d}\zeta_{ba} \int (2j_{ab} + 1) \mathrm{d}\tilde{\zeta}_{ab} \int (2j_{ab} + 1) \mathrm{d}\tilde{\zeta}_{ba}
$$

$$
\times (2j_{ab} + 1) \int \mathrm{d}z_{ab} \frac{[\zeta_{ba}|z_{ab}\rangle^{2j_{ab}} \langle z_{ab}|g_{ab}|\zeta_{ab}\rangle^{2j_{ab}}}{\|z_{ab}\|^{2j_{ab}+2i\gamma j_{ab}+2} \|g_{ab}^\dagger z_{ab}\|^{2j_{ab}-2i\gamma j_{ab}+2}} \langle \zeta_{ab}|\tilde{\zeta}_{ab}]^{2j_{ab}}
$$

$$
\times (2j_{ab} + 1) \int \mathrm{d}\tilde{z}_{ba} \frac{[\tilde{\zeta}_{ab}|\tilde{z}_{ba}\rangle^{2j_{ab}} \langle \tilde{z}_{ba}|\tilde{g}_{ba}|\tilde{\zeta}_{ba}\rangle^{2j_{ab}}}{\|\tilde{z}_{ba}\|^{2j_{ab}+2i\gamma j_{ab}+2} \|\tilde{g}_{ba}^\dagger \tilde{z}_{ba}\|^{2j_{ab}-2i\gamma j_{ab}+2}} \langle \tilde{\zeta}_{ba}|\zeta_{ba}]^{2j_{ab}}. \tag{D1}
$$

We group the integrations over the various spinors under a single symbol $d\Omega$, and we collect the integer $2j_{ab}$ from the exponent

$$
F_{\mathrm{EPRL}}(g_{ab}, \tilde{g}_{ba}) = \sum_{j_{ab}} (2j_{ab} + 1)^7 \int d\Omega (f_{\mathrm{EPRL}}(g_{ab}, \tilde{g}_{ba}))^{j_{ab}}, \tag{D2}
$$

where we denoted with

$$
f_{\mathrm{EPRL}}(g_{ab}, \tilde{g}_{ba}) = \frac{[\zeta_{ba}|z_{ab}\rangle \langle z_{ab}|g_{ab}|\zeta_{ab}\rangle}{\|z_{ab}\|^{1+i\gamma} \|g_{ab}^\dagger z_{ab}\|^{1-i\gamma}} \langle \zeta_{ab}|\tilde{\zeta}_{ab}] \frac{[\tilde{\zeta}_{ab}|\tilde{z}_{ba}\rangle \langle \tilde{z}_{ba}|\tilde{g}_{ba}|\tilde{\zeta}_{ba}\rangle}{\|\tilde{z}_{ba}\|^{1+i\gamma} \|\tilde{g}_{ba}^\dagger \tilde{z}_{ba}\|^{1-i\gamma}} \langle \tilde{\zeta}_{ba}|\zeta_{ba}]. \tag{D3}
$$

We recast the sum over half-integer spins in terms of integers since $2j_{ab} \in \mathbb{N}$. The function $F_{\mathrm{EPRL}}(g_{ab}, \tilde{g}_{ba})$ has the form of (the seventh derivative of) a geometric series that is defined in the whole complex plane but 1, where it is singular. Therefore we find the singular support of (D2) for values of the holonomies such that $w_{\mathrm{EPRL}}(g_{ab}, \tilde{g}_{ba}) = 1$ or

$$
\frac{[\zeta_{ba}|z_{ab}\rangle \langle z_{ab}|g_{ab}|\zeta_{ab}\rangle}{\|z_{ab}\|^{1+i\gamma} \|g_{ab}^\dagger z_{ab}\|^{1-i\gamma}} \langle \zeta_{ab}|\tilde{\zeta}_{ab}] \frac{[\tilde{\zeta}_{ab}|\tilde{z}_{ba}\rangle \langle \tilde{z}_{ba}|\tilde{g}_{ba}|\tilde{\zeta}_{ba}\rangle}{\|\tilde{z}_{ba}\|^{1+i\gamma} \|\tilde{g}_{ba}^\dagger \tilde{z}_{ba}\|^{1-i\gamma}} \langle \tilde{\zeta}_{ba}|\zeta_{ba}] = 1. \tag{D4}
$$

Note that we are integrating all the spinors. In general, there are no holonomies such that (D4) is satisfied. Taking the absolute value of the left-hand side of the (D4) and applying the Cauchy-Schwarz inequality to all the scalar products at the numerator

$$
|f_{\mathrm{EPRL}}(g_{ab}, \tilde{g}_{ba})| = \left| \frac{[\zeta_{ba}|z_{ab}\rangle \langle z_{ab}|g_{ab}|\zeta_{ab}\rangle}{\|z_{ab}\| \|g_{ab}^\dagger z_{ab}\|} \langle \zeta_{ab}|\tilde{\zeta}_{ab}] \frac{[\tilde{\zeta}_{ab}|\tilde{z}_{ba}\rangle \langle \tilde{z}_{ba}|\tilde{g}_{ba}|\tilde{\zeta}_{ba}\rangle}{\|\tilde{z}_{ba}\| \|\tilde{g}_{ba}^\dagger \tilde{z}_{ba}\|} \langle \tilde{\zeta}_{ba}|\zeta_{ba}] \right| \leq 1. \tag{D5}
$$

The inequality is saturated if all the vectors in the scalar product are proportional, in particular, if for some real parameters $\rho_i \in \mathbb{R}$ and $\beta_i \in \mathbb{R}$

$$
|z_{ab}\rangle = e^{i\beta_1}|\zeta_{ba}] \quad g_{ab}|\zeta_{ab}\rangle = e^{\rho_2+i\beta_2}|z_{ab}] \quad |\tilde{\zeta}_{ab}] = e^{i\beta_3}|\zeta_{ab}\rangle
$$
$$
|\tilde{z}_{ba}\rangle = e^{i\beta_4}|\tilde{\zeta}_{ab}] \quad \tilde{g}_{ba}|\tilde{\zeta}_{ba}\rangle = e^{\rho_5+i\beta_5}|\tilde{z}_{ba}\rangle \quad |\zeta_{ba}] = e^{i\beta_6}|\tilde{\zeta}_{ba}\rangle. \tag{D6}
$$

Combining Eq. (D6) we find an eigenvalue equations for the face holonomy

$$
\tilde{g}_{ba} g_{ab}|\zeta_{ab}\rangle = e^{\frac{\omega_f}{2}}|\zeta_{ab}\rangle, \tag{D7}
$$

where $\frac{\omega_f}{2} = \rho_2 + \rho_5 + i(\beta_1 + \beta_2 + \beta_3 + \beta_4 + \beta_5 + \beta_6)$. From the Cauchy-Schwarz inequality we also get the extra equations

$$
|\zeta_{ab}\rangle = e^{\rho_7 - i\beta_7}(g_{ab}^\dagger)^{-1}|z_{ab}\rangle \quad |\tilde{\zeta}_{ba}\rangle = e^{\rho_8 - i\beta_8}(\tilde{g}_{ba}^\dagger)^{-1}|\tilde{z}_{ba}\rangle, \tag{D8}
$$

or equivalently

$$g_{ab}|\zeta_{ab}] = e^{\rho_7 + i\beta_7}|z_{ab}] \quad \tilde{g}_{ba}|\tilde{\zeta}_{ba}\rangle = e^{\rho_8 + i\beta_8}|\tilde{z}_{ba}\rangle. \tag{D9}$$

From these equations we find that also $|\zeta_{ab}]$ is an eigenvector of the face holonomy

$$\tilde{g}_{ba}g_{ab}|\zeta_{ab}] = e^{\frac{\tilde{\omega}_f}{2}}|\zeta_{ab}]. \tag{D10}$$

From the orthonormality of the eigenvectors and det $\tilde{g}_{ba}g_{ab} = 1$ we conclude that $\tilde{\omega}_f = -\omega_f$. We insert Eqs. (D6) and (D8) into (D4) to derive a condition on the real and imaginary part of the face complex angle

$$\frac{\gamma \mathrm{Re}\omega_f + \mathrm{Im}\omega_f}{2} = 0 \bmod 2\pi \quad \text{or} \quad \gamma \mathrm{Re}\omega_f + \mathrm{Im}\omega_f = 4k\pi \quad k \in \mathbb{Z}. \tag{D11}$$

Since we are integrating over $|\zeta_{ab}\rangle$ we can conclude that $\tilde{g}_{ba}g_{ab}$ can be an arbitrary 4-screw with the relation (D11) between rapidity and rotation angle.

$$\mathrm{Sing}(F_{\mathrm{EPRL}}(g_{ab}, \tilde{g}_{ba})) = \{g_{ab}, \tilde{g}_{ba}|\tilde{g}_{ba}g_{ab} = e^{\frac{\omega_f}{2}}|\zeta\rangle\langle\zeta| + e^{-\frac{\omega_f}{2}}|\zeta][\zeta| \text{ with } \gamma \mathrm{Re}\omega_f + \mathrm{Im}\omega_f = 0 \bmod 4\pi\}. \tag{D12}$$

The calculation for a general face with any amount of wedges (vertices) is the same. For example, the singular support of the EPRL function associated with a face with $1, \dots, n$ wedges is

$$\mathrm{Sing}(F_{\mathrm{EPRL}}(g_1, \dots, g_n)) = \{(g_1, \dots, g_n)|g_f = e^{\frac{\omega_f}{2}}|\zeta\rangle\langle\zeta| + e^{-\frac{\omega_f}{2}}|\zeta][\zeta| \text{ with } \gamma \mathrm{Re}\omega_f + \mathrm{Im}\omega_f = 0 \bmod 4\pi\}, \tag{D13}$$

where $g_f = g_n \cdots g_1$ is just the (ordered) product of all the wedge holonomies belonging to that face.

---

[1] J. Engle, E. Livine, R. Pereira, and C. Rovelli, LQG vertex with finite Immirzi parameter, Nucl. Phys. **B799**, 136 (2008).

[2] L. Freidel and K. Krasnov, A new spin foam model for 4D gravity, Classical Quantum Gravity **25**, 125018 (2008).

[3] C. Rovelli and F. Vidotto, *Covariant Loop Quantum Gravity: An Elementary Introduction to Quantum Gravity and Spinfoam Theory*, Cambridge Monographs on Mathematical Physics (Cambridge University Press, Cambridge, England, 2014).

[4] A. Perez, The spin foam approach to quantum gravity, Living Rev. Relativity **16**, 3 (2013).

[5] J. W. Barrett, R. J. Dowdall, W. J. Fairbairn, F. Hellmann, and R. Pereira, Lorentzian spin foam amplitudes: Graphical calculus and asymptotics, Classical Quantum Gravity **27**, 165009 (2010).

[6] J. W. Barrett, R. J. Dowdall, W. J. Fairbairn, H. Gomes, and F. Hellmann, Asymptotic analysis of the EPRL four-simplex amplitude, J. Math. Phys. (N.Y.) **50**, 112504 (2009).

[7] J. W. Barrett, W. J. Fairbairn, and F. Hellmann, Quantum gravity asymptotics from the SU(2) 15j symbol, Int. J. Mod. Phys. A **25**, 2897 (2010).

[8] P. Donà, M. Fanizza, G. Sarno, and S. Speziale, SU(2) graph invariants, Regge actions and polytopes, Classical Quantum Gravity **35**, 045011 (2018).

[9] W. Kaminski, M. Kisielowski, and J. Lewandowski, Spin-foams for all loop quantum gravity, Classical Quantum Gravity **27**, 095006 (2010); **29**, 049502(E) (2012).

[10] P. Dona and S. Speziale, Asymptotics of lowest unitary SL(2, C) invariants on graphs, Phys. Rev. D **102**, 086016 (2020).

[11] P. Dona, M. Fanizza, P. Martin-Dussaud, and S. Speziale, Asymptotics of SL(2, $\mathbb{C}$) coherent invariant tensors, Commun. Math. Phys. **389**, 399 (2022).

[12] P. Donà, M. Fanizza, G. Sarno, and S. Speziale, Numerical study of the Lorentzian Engle-Pereira-Rovelli-Livine spin foam amplitude, Phys. Rev. D **100**, 106003 (2019).

[13] F. Gozzini, A high-performance code for EPRL spin foam amplitudes, Classical Quantum Gravity **38**, 225010 (2021).

[14] J. W. Barrett and L. Crane, Relativistic spin networks and quantum gravity, J. Math. Phys. (N.Y.) **39**, 3296 (1998).

[15] G. Immirzi, Quantum gravity and Regge calculus, Nucl. Phys. B, Proc. Suppl. **57**, 65 (1997).

[16] J. W. Barrett and R. M. Williams, The asymptotics of an amplitude for the four simplex, Adv. Theor. Math. Phys. **3**, 209 (1999).

[17] B. Dittrich and J. P. Ryan, Phase space descriptions for simplicial 4d geometries, Classical Quantum Gravity **28**, 065006 (2011).

[18] L. Freidel and S. Speziale, Twisted geometries: A geometric parametrisation of SU(2) phase space, Phys. Rev. D **82**, 084040 (2010).

[19] L. Freidel and J. Hnybida, A discrete and coherent basis of intertwiners, Classical Quantum Gravity **31**, 015019 (2014).

[20] S. Speziale and W. M. Wieland, The twistorial structure of loop-gravity transition amplitudes, Phys. Rev. D **86**, 124023 (2012).

[21] F. Anzà and S. Speziale, A note on the secondary simplicity constraints in loop quantum gravity, Classical Quantum Gravity **32,** 195015 (2015).

[22] S. K. Asante, J. D. Simão, and S. Steinhaus, Spin-foams as semiclassical vertices: Gluing constraints and a hybrid algorithm, Phys. Rev. D **107,** 046002 (2023).

[23] F. Hellmann and W. Kaminski, Holonomy spin foam models: Asymptotic geometry of the partition function, J. High Energy Phys. 10 (2013) 165.

[24] C. Rovelli and S. Speziale, On the geometry of loop quantum gravity on a graph, Phys. Rev. D **82,** 044018 (2010).

[25] L. Freidel and S. Speziale, From twistors to twisted geometries, Phys. Rev. D **82,** 084041 (2010).

[26] M. Dupuis, J. P. Ryan, and S. Speziale, Discrete gravity models and Loop quantum gravity: A short review, SIGMA **8,** 052 (2012).

[27] Y. Ding, M. Han, and C. Rovelli, Generalized Spinfoams, Phys. Rev. D **83,** 124020 (2011).

[28] B. Bahr, Non-convex 4d polytopes in Spin Foam Models, 2018.

[29] B. Dittrich and S. Speziale, Area-angle variables for general relativity, New J. Phys. **10,** 083006 (2008).

[30] B. Dittrich and J. P. Ryan, Simplicity in simplicial phase space, Phys. Rev. D **82,** 064026 (2010).

[31] M. Långvik and S. Speziale, Twisted geometries, twistors and conformal transformations, Phys. Rev. D **94,** 024050 (2016).

[32] P. Dona and G. Sarno, Numerical methods for EPRL spin foam transition amplitudes and Lorentzian recoupling theory, Gen. Relativ. Gravit. **50,** 127 (2018).

[33] E. R. Livine, Deformations of polyhedra and polygons by the unitary group, J. Math. Phys. (N.Y.) **54,** 123504 (2013).

[34] E. Bianchi, D. Regoli, and C. Rovelli, Face amplitude of spinfoam quantum gravity, Classical Quantum Gravity **27,** 185009 (2010).

[35] J. Engle and R. Pereira, Regularization and finiteness of the Lorentzian LQG vertices, Phys. Rev. D **79,** 084034 (2009).

[36] M. Han and M. Zhang, Asymptotics of spinfoam amplitude on simplicial manifold: Lorentzian theory, Classical Quantum Gravity **30,** 165012 (2013).

[37] M.-X. Han and M. Zhang, Asymptotics of spinfoam amplitude on simplicial manifold: Euclidean theory, Classical Quantum Gravity **29,** 165004 (2012).

[38] W. Kaminski and H. Sahlmann, The hessian in spin foam models, Ann. Inst. Henri Poincaré **20,** 3927 (2019).

[39] G. P. Ponzano and T. E. Regge, Semiclassical limit of racah coefficients, in *Spectroscopy and Group Theoretical Methods in Physics* (Elsevier, 1968), pp. 1–58.

[40] P. Donà, F. Gozzini, and G. Sarno, Searching for classical geometries in spin foam amplitudes: A numerical method, Classical Quantum Gravity **37,** 094002 (2020).

[41] F. Conrady and L. Freidel, On the semiclassical limit of 4d spin foam models, Phys. Rev. D **78,** 104023 (2008).

[42] V. Bonzom, Spin foam models for quantum gravity from lattice path integrals, Phys. Rev. D **80,** 064028 (2009).

[43] M. Han, Semiclassical analysis of spinfoam model with a small Barbero-Immirzi parameter, Phys. Rev. D **88,** 044051 (2013).

[44] J. S. Engle, W. Kaminski, and J. R. Oliveira, Addendum to 'EPRL/FK asymptotics and the flatness problem', Classical Quantum Gravity **38,** 119401(A) (2021).

[45] S. K. Asante, B. Dittrich, and H. M. Haggard, Discrete gravity dynamics from effective spin foams, Classical Quantum Gravity **38,** 145023 (2021).

[46] S. K. Asante, B. Dittrich, and J. Padua-Arguelles, Effective spin foam models for Lorentzian quantum gravity, Classical Quantum Gravity **38,** 195002 (2021).